Technetium-99m Labeled to Human Immunoglobulin G Through the Nicotinyl Hydrazine Derivative: A Clinical Study

Els T.M. Dams, Wim J.G. Oyen, Otto C. Boerman, Roel A.M.J. Claessens, Ate B. Wymenga, Jos W.M. van der Meer and Frans H.M. Corstens

Departments of Nuclear Medicine and Internal Medicine, University Hospital Nijmegen, and Department of Orthopedics, St. Maartenskliniek, Nijmegen, The Netherlands

A novel method to label polyclonal human immunoglobulin G (IgG) with ^{99m}Tc through the nicotinyl hydrazine derivative (HYNIC) has shown promising results in the detection of experimental infection. In this study, ^{99m}Tc-labeled HYNIC–IgG was directly compared to ^{111}In-labeled diethylenetriaminepentaacetic acid (DTPA)–IgG in patients suspected of infectious or inflammatory disease. **Methods:** Thirty-seven patients (22 women and 15 men; mean age = 54 yr, range = 17–78 yr) with 39 suspected infectious or inflammatory foci were prospectively studied. After administration of 740 MBq ^{99m}Tc-HYNIC–IgG, imaging was performed at 4 and 24 hr postinjection. To avoid cross-over activity, ^{111}In-DTPA–IgG was injected 24 hr after ^{99m}Tc-HYNIC–IgG and imaged at 4, 24 and 48 hr postinjection. The scintigraphic results were confirmed by microbiological, histological, radiological and clinical methods. **Results:** Technetium-99m-HYNIC–IgG and ^{111}In-DTPA–IgG scintigraphy showed 100% concordancy. All 17 patients with proven infection or inflammation (19 foci, mainly localized in the locomotor system) had positive scintigraphic findings. No false-negative scintigrams were recorded. In three patients, the scintigrams were concordantly false-positive. As a result, the sensitivity and specificity of imaging infectious or inflammatory foci with ^{99m}Tc-HYNIC–IgG and ^{111}In-DTPA–IgG in these patients were 100% and 85%, respectively. **Conclusion:** Technetium-99m-HYNIC–IgG scintigraphy is equally as effective as ^{111}In–IgG scintigraphy for the detection of infection and inflammation. The apparent physical and logistic advantages of ^{99m}Tc over ^{111}In make ^{99m}Tc-HYNIC–IgG a promising new radiopharmaceutical for imaging infection and inflammation.

Key Words: infection; inflammation; immunoglobulin G; HYNIC; imaging

J Nucl Med 1998; 39:119–124

Rapid and accurate localization of infectious and inflammatory foci has significant impact on the therapeutic management of patients suspected of having such disease entities. Several scintigraphic techniques have been developed to detect infection and inflammation. The most commonly used radiopharmaceuticals are ^{67}Ga-citrate (*1,2*), ^{111}In-labeled leukocytes (*3–5*) and ^{99m}Tc-labeled leukocytes (*6,7*). These agents, however, have various limitations. The accumulation of ^{67}Ga-citrate in the bowel, in areas of bone remodeling and in malignancies, limits its usefulness in detecting infection (*8–12*). The unfavorable physical properties of ^{67}Ga result in impaired image quality and a high radiation burden for the patient. The labeling of leukocytes is complicated and time-consuming and has an inherent risk of blood-borne infections to patients and staff (*13*). Moreover, leukocytes cannot be used in neutropenic patients.

A recently introduced scintigraphic technique, using ^{111}In-labeled human nonspecific immunoglobulin G (IgG), has shown promising results in the evaluation of infectious and inflammatory diseases (*14,15*) and lacks many of these disadvantages. The radiopharmaceutical is easily prepared and safe. In addition, the sensitivity and specificity for the detection of infectious and inflammatory foci in normal and immunocompromised patients is high (*16–18*). At present, ^{111}In–IgG is routinely used in our department for infection imaging. However, ^{111}In is not an ideal radionuclide. It is relatively expensive and has limited availability and suboptimal imaging characteristics, and its radiation dose is not particularly low. A ^{99m}Tc conjugate would be more appealing for logistic, economic and dosimetric reasons. However, many of the existing methods of labeling ^{99m}Tc to IgG are either complicated (*19*) or result in marked in vivo instability, influencing the biodistribution of ^{99m}Tc (*20,21*). A recently developed indirect method of labeling IgG with ^{99m}Tc through a nicotinyl hydrazine derivative (HYNIC) has shown an in vivo behavior that is similar to that of ^{111}In-DTPA–IgG in experimental infection (*22,23*).

In this prospective study, we compared the clinical efficacy of ^{99m}Tc-HYNIC–IgG and ^{111}In-DTPA–IgG in patients referred for infection/inflammation imaging.

MATERIALS AND METHODS

Study Design

This prospective, comparative study was performed with 37 patients (22 women and 15 men; mean age = 54 yr, range = 17–78 yr) who were referred to the department of nuclear medicine of University Hospital Nijmegen for infection scanning. Technetium-99m-HYNIC–IgG scintigraphy was performed first, and ^{111}In-diethylenetriaminepentaacetic acid (DTPA)–IgG scintigraphy was performed 24 hr later. In six patients, serial blood samples were taken after ^{99m}Tc–IgG injection to measure the blood clearance of ^{99m}Tc-HYNIC–IgG. Informed consent was obtained from the patient and the referring physician. The study protocol was approved by the Ethical Review Board of the University Hospital Nijmegen.

The 37 patients included in the study had 39 possible infectious or inflammatory foci. Seventeen patients were suspected of joint prosthesis infection. Nine patients were referred for suspected bone infection, and one of them also had possible soft-tissue and hip prosthesis infection. Two patients were suspected of spondylodiscitis. Six patients had fever of unknown origin. Two patients had had unexplained bacteremia, and one patient had possible pulmonary sarcoidosis.

The scintigraphic results were verified by the following procedures: culture of a sample obtained by surgery (n = 15), by fine-needle aspiration (n = 5) or from body fluids (n = 5); histological examination of a biopsy (n = 2); roentgenology (n = 13) and MRI (n = 5); and clinical follow-up of at least 6 mo (n = 20). Follow-up implied the absence of signs or symptoms of

Received Dec. 23, 1996; revision accepted Mar. 25, 1997.

For correspondence or reprints contact: E.Th., M. Dams, MD, Department of Internal Medicine, University Hospital, P.O. Box 9101, 6500 HB Nijmegen, The Netherlands.

infection/inflammation in patients with negative scintigraphic findings or a favorable response to installed treatment, confirming positive scintigraphic results. In all patients in whom the scintigraphic results were not confirmed at surgery, at least two confirmation procedures were performed.

Radiopharmaceuticals

Indium-111–Immunoglobulin G. Diethylenetriaminepentaacetic acid bicyclic anhydride (bicyclic DTPA) was conjugated to human immunodeficiency virus and hepatitis B surface antigen-negative, human, nonspecific, polyclonal IgG (Gammagard; Baxter/Hyland, Lessines, Belgium) and radiolabeled with ^{111}In (^{111}In-chloride; Mallinckrodt, Inc., Petten, The Netherlands) through citrate transchelation. Two to three DTPA ligands were present per IgG molecule. The labeling efficiency was always higher than 95%. A dose of approximately 2 mg of IgG labeled with 75 MBq ^{111}In was injected intravenously.

Technetium-99m–Immunoglobulin G. The HYNIC was synthesized and conjugated to human polyclonal IgG (Gammagard) according to the method described by Abrams et al. (*22*). Approximately three HYNIC groups were coupled per IgG molecule. The purified HYNIC-conjugated IgG was diluted to 4 mg/ml with 0.15 *M* acetate (pH 5.85), sterilized by membrane filtration and stored at −20°C in 0.5-ml aliquots. After thawing 0.5 ml of the HYNIC–IgG conjugate, the conjugate was radiolabeled with ^{99m}Tc by the addition of 0.1 mg N-[Tris(hydroxymethyl)-methyl]glycine (Tricine; Sigma Chemical Company, St. Louis, MO), 0.01 mg $SnSO_4$ and 740 MBq ^{99m}Tc-pertechnetate. The mixture was incubated for 15 min at room temperature. The radiochemical purity was determined by instant thin-layer chromatography (ITLC) (Gelman, Ann Arbor, MI) with 0.15 *M* acetate (pH 5.85) as the mobile phase. Labeling efficiency was always higher than 95%. A dose of 2 mg IgG labeled with approximately 740 MBq ^{99m}Tc was injected intravenously.

Imaging Protocol and Image Interpretation

Scintigraphic images were obtained with a Siemens Orbiter or MultiSpect 2 gamma camera, connected to a Scintiview image processor and ICON computer system (Siemens Inc., Hoffman Estates, IL). All images were collected in digital format in a 256 × 256 matrix. Spot views of ^{99m}Tc–IgG were acquired at 4 hr postinjection for a preset time of 5 min, using a low-energy, parallel-hole collimator (140-keV photopeak, 15% symmetric window). After 24 hr, whole-body scans were recorded (scan speed, 7 cm/min). To avoid cross-over activity, ^{111}In–IgG was administered 24 hr after the administration of ^{99m}Tc–IgG and imaged at 4, 24 and 48 hr postinjection with preset times of 5, 7.5 and 10 min, respectively, using a medium-energy, parallel-hole collimator (173-keV peak, 15% symmetric window; and 247-keV peak, 15% symmetric window). Phantom studies proved the scatter of ^{99m}Tc on the ^{111}In recordings 4 hr postinjection to be less than 1%.

Images were interpreted separately by two independent observers, who were blinded to the results of the verification procedures. Disagreements were settled by consensus. Both ^{99m}Tc–IgG and ^{111}In–IgG scans were considered positive for inflammation or infection when focal accumulation of tracer with time was observed. All other scintigrams were considered negative, including those with known causes of nonpathological uptake, such as in the synovial lining of total knee prostheses and around the neck of total hip prostheses without osseous involvement (*24*).

RESULTS

The biodistribution of ^{99m}Tc-HYNIC–IgG in this group of patients was very similar to the distribution of ^{111}In-DTPA–IgG. There was marked uptake in the cardiac blood pool, liver and spleen and, to a lesser degree, in the kidneys. Uptake was low in lung, bone, muscle and gastrointestinal tract (Fig. 1). A relatively high intravascular activity of ^{99m}Tc-HYNIC–IgG could be noted up to 24 hr postinjection Figure 2 shows the blood clearance curve for ^{99m}Tc-HYNIC–IgG in six patients. The $t_{1/2}$ of the alpha phase of the blood clearance, calculated from these data, was 1.8 ± 0.8 hr, and the $t_{1/2}$ of the beta phase was 53.6 ± 10.3 hr.

FIGURE 1. Anterior and posterior whole-body ^{99m}Tc-HYNIC–IgG scintigram showing normal distribution of the radiolabel at 24 hr postinjection

A summary of the patients, their scintigraphic results and the verification procedures is provided in Table 1. Examples of abnormal ^{99m}Tc–IgG and ^{111}In–IgG scans are shown in Figures 3 and 4. The results of ^{99m}Tc-HYNIC–IgG and ^{111}In-DTPA–IgG scintigraphies were 100% concordant. No focal infection was missed by either of the techniques. Of the 37 patients, 17 had proven infection or inflammation (Patients 1–17 in Table 1). A positive culture was obtained in 12 of the 14 patients with infection; all infections were located in the locomotor system. In two patients (Patients 13 and 14), culture results were unavailable. Patient 13, with accumulation of IgG in the pubic bone region, was diagnosed as having acute pubic bone osteo-

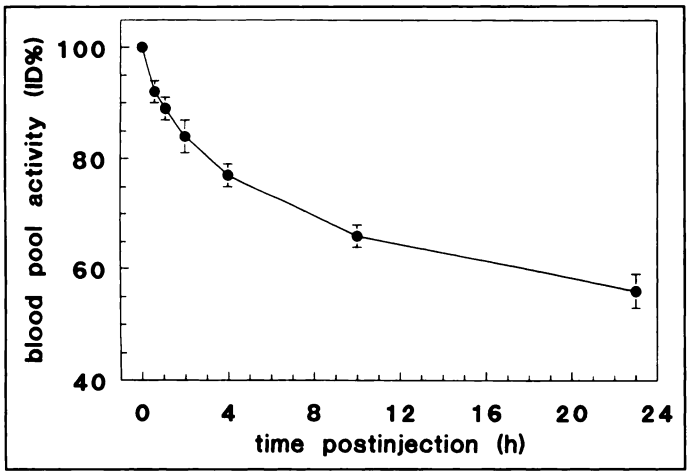

FIGURE 2. Blood clearance of ^{99m}Tc-HYNIC–IgG in six patients. Blood-pool activity measured 5 min postinjection was set at 100%. Error bars represent s.e.m.

myelitis, in accordance with the clinical findings. She responded favorably to a long-term course of flucloxacillin. Patient 14 was suspected of reinfection several months after removal of infected external fixation material from the right tibia. Both studies showed increased uptake at the anterior side of the tibia. At surgery, pus was seen, corresponding with the infection, as depicted on the scintigrams. The causative microorganism was not identified.

Three patients (Patients 15–17) with concordantly true-positive scans had noninfectious inflammatory disease. One patient (Patient 15), who had a 6-mo history of fever, fatigue and lower back pain, elevated erythrocyte sedimentation rate and positive serology for *Yersinia enterocolitica*, had symmetrically increased activity in the sacroiliacal region. *Yersinia*-related reactive sacroiliitis was diagnosed. Treatment with nonsteroidal anti-inflammatory drugs resulted in rapid clinical and hematological improvement. In the second patient (Patient 16), who had unexplained fever for 1 wk after neurosurgery, IgG accumulation was seen in the course of the right femoral vein. The presumptive diagnosis of femoral vein thrombosis was subsequently confirmed by ultrasound. She responded well to anticoagulant therapy. The third patient (Patient 17) had mild leukocytosis for 3 yr and complained of fatigue and headache. His pulmonary tests revealed a marked reduction in diffusion capacity, indicative of possible pulmonary sarcoidosis. Both scans showed enhanced pulmonary uptake, but bronchoalveolar lavage and high-resolution CT scan of the lungs were normal. A lung biopsy, however, histologically showed an interstitial pneumonitis, possibly related to beryllium exposure, thus confirming the scintigraphic results.

Concordantly false-positive scintigrams were obtained in three patients (Patients 18–20). One patient (Patient 18), who had an 18-mo history of periodic high fever, had increased IgG uptake in the prostate region, suggesting prostatitis. Cultures, however, remained sterile. A prostate biopsy revealed a low-grade adenocarcinoma. No signs of metastatic disease were seen on MRI, and treatment was deferred. The recurrent febrile episodes remained unexplained. In the second patient (Patient 19), the enhanced uptake in the lungs on both the ^{99m}Tc and ^{111}In scans could not be verified. She had a history of long-standing fever, although this was not confirmed during clinical observation elsewhere. At the time of the scintigraphic procedure, she complained of a slight productive cough. A chest radiograph, which had limited reliability because of her extreme obesity, showed no abnormalities. A CT scan of the lungs also was normal, but at that time, 6 wk after the scintigraphic procedures, the cough had subsided. The third patient (Patient 20), who had false-positive scintigraphic findings, had possible septical loosening of his 12-yr-old cemented hip prosthesis. Both scintigrams revealed increased accumulation at the neck of the femoral component, but at surgery, no infection was detected and cultures remained sterile. Replacement of the prosthesis resulted in immediate clinical improvement.

The two patients with unexplained bacteremia (Patients 21 and 22) were considered to be true-negative. Both patients had been treated with antibiotics for several weeks before referral for imaging, their cultures at time of imaging remained sterile and subsequent evaluation and clinical follow-up failed to identify an infectious focus. Patients 23 and 34, who had fever of unknown origin, were interpreted also as true-negative because of the negative microbiological and radiological findings and the diminution of the fever without antibiotic treatment.

In view of the concordant results, ^{99m}Tc-HYNIC–IgG and ^{111}In–IgG scintigraphies yielded the same sensitivity and specificity in this group of patients. For the overall group, the figures were 100% (17 of 17) and 85% (17 of 20), respectively, on a patient basis. For focal sites of infection/inflammation (joint prosthesis and bone and soft tissue infection), the specificity was 93% (13 of 14).

DISCUSSION

This study indicates that ^{99m}Tc-HYNIC–IgG scintigraphy performs equally as well as ^{111}In–IgG scintigraphy in this group of patients with nonacute infections. The infections were mainly localized in the peripheral locomotor system. Technetium-99m-HYNIC–IgG accurately depicted all infectious and inflammatory foci, including chronic osteomyelitis, spondylodiscitis and pulmonary inflammation. The excellent performance of ^{111}In–IgG in delineating locomotor infections (*25*) was confirmed in our study. No infections were missed by either of the techniques, resulting in a sensitivity of 100%. The specificity of 85% reflects the nonspecific nature of radiolabeled IgG, accumulating at sites of both infection and inflammation (*16*). This is illustrated by our false-positive results. Uptake of ^{99m}Tc–IgG and ^{111}In–IgG in prostatic cancer (Patient 18) may reflect inflammatory activity around a malignancy, as previously reported in the literature (*14,26*). Radiolabeled IgG has even been suggested to be helpful in the evaluation of certain cancers (*27*). However, we could not attribute the fever to the finding of prostatic cancer, and the result was classified as false-positive. Uptake due to noninfectious inflammation also can be noted in total hip arthroplasties, mainly within the first 14 mo after implantation of a cementless arthroplasty (*24*). In addition, periarticular ossification and wear of the socket, both regularly causing sterile inflammatory reactions, are potential pitfalls in image interpretation (*24*). Noninfectious inflammation probably caused the false-positive result in Patient 20 with a total hip prosthesis. The false-positive result in Patient 19 remains unexplained but could be due to an unconfirmed pulmonary infection. Increased IgG uptake in the joints of patients with rheumatoid arthritis, as in Patient 9, could represent disease activity and incorrectly be interpreted as septic arthritis. However, in most cases, the pattern and intensity of IgG uptake is very different: diffuse, intense uptake is seen in the joint in septic arthritis, whereas in rheumatoid arthritis, the synovial lining is typically visualized (*24*). Information on clinical presentation further contributes to a correct interpretation, which can be confirmed by cultures (as in Patient 9).

Specificity values are clearly influenced by the interpretation

TABLE 1
Clinical Characteristics and Results of Scintigraphy and Verification Procedures

Patient no.	Sex	Age (yr)	Duration	Suspected focus	Scintigraphy		Verification		Assessment
					^{111}In–IgG	^{99m}Tc–IgG	Procedure	Result	
1	F	65	8 mo	Total knee prosthesis	+	+	S	SE infection	TP
2	M	45	2 mo	Foot	+	+	S	PM osteomyelitis	TP
3	F	66	5 mo	Total hip prosthesis	+	+	S	SH infection	TP
4	F	70	2 mo	Total hip prosthesis	+	+	P, R, FU	SAn infection	TP
5	F	22	2 mo	Treated SA bacteremia lumbar spine	+	+	MRI, FU	SA spondylodiscitis	TP
6	F	69	1 yr	Total hip prosthesis	+	+	S	SA infection	TP
7	M	58	1 yr	Total hip prosthesis	+	+	S	SH infection	TP
8	M	57	17 yr	Femur	+	+	S	SA osteomyelitis	TP
9	F	40	2 wk	Total hip prosthesis	+	+	F	SA infection	TP
				Ankle	+	+	P	SA infection	TP
				Foot	+	+	P	SA infection	TP
10	M	76	2 wk	Total hip prosthesis	+	+	S	SA infection	TP
11	F	66	1 wk	Girdlestone hip	+	+	S	PA soft-tissue infection (productive fistula)	TP
12	M	69	8 mo	Total hip prosthesis	+	+	S	SE infection	TP
13	F	36	1 wk	Pubic bone	+	+	R, FU	Osteomyelitis of pubic bone	TP
14	F	21	3 wk	Tibia	+	+	S	Soft-tissue infection	TP
15	F	42	6 mo	Fever of unknown origin	+	+	MRI, FU	Yersinia-related sacroiliitis	TP
16	F	49	1 wk	Fever of unknown origin	+	+	R, FU	Femoral vein trombosis	TP
17	M	36	3 yr	Lung	+	+	B	Interstitial pneumonitis	TP
18	M	68	2 yr	Fever of unknown origin	+	+	B, MRI, FU	Prostatic cancer; fever unexplained	FP
19	F	39	1 yr	Fever of unknown origin	+	+	C, R, FU	No cause identified	FP
20	M	53	4 mo	Total hip prosthesis	+	+	S	Aseptical loosening; no infection	FP
21	M	64	4 wk	Treated EC bacteremia	−	−	C, R, FU	No cause identified	TN
22	M	54	2 wk	Treated SA bacteremia	−	−	C, R, FU	No evidence of persisting infection	TN
23	M	38	9 mo	Fever of unknown origin	−	−	C, R, FU	No cause identified; fever subsided	TN
24	F	44	2 yr	Lumbar spine	−	−	MRI, FU	No evidence of infection	TN
25	F	76	1 yr	Total knee prosthesis	−	−	P, FU	Osteoarthritis; no infection proven	TN
26	F	61	1 yr	Total knee prosthesis	−	−	R, FU	No infection proven	TN
27	M	59	4 mo	Total hip prosthesis	−	−	S	No infection	TN
28	M	70	4 mo	Femur	−	−	R, FU	No infection proven	TN
29	M	17	2 yr	Knee	−	−	P, MRI, FU	Noninfected osteoarthritis	TN
30	F	43	9 mo	Tibia	−	−	S	Pseudoarthrosis; no infection	TN
31	M	33	5 yr	MTP I	−	−	S	Pseudoarthrosis; no infection	TN
32	F	66	8 mo	Total hip prosthesis	−	−	S	Loosening prosthesis; no infection	TN
33	F	68	1 yr	Total hip prosthesis	−	−	S	Loosening prosthesis; no infection	TN
34	F	45	4 wk	Fever of unknown origin	−	−	C, R, FU	No cause identified; fever subsided	TN
35	F	78	1 yr	Total hip prosthesis	−	−	R, FU	Protruding acetabulum; no infection proven	TN
36	F	75	2 mo	Total hip prosthesis	−	−	R, FU	Loosening prosthesis; no infection proven	TN
37	F	69	1 yr	Total knee prosthesis	−	−	R, FU	No infection proven	TN

C = bacterial culture; P = puncture; B = biopsy; R = roentgenologic procedures; FU = clinical follow-up of at least 6 mo; S = surgery; SE = *Staphylococcus epidermis*; PM = *Pasteurella multocida*; SAn = *Streptococcus anginosus*; SA = *Staphylococcus aureus*; PA = *Pseudomonas aeruginosa*; EC = *Escherichia coli*; SH = *Streptococcus haemolyticus*; TP = true-positive; TN = true-negative; FP = false-positive.

of the scintigraphy and the definition of false-positivity. The results of the scintigrams were classified according to the clinical context and therapeutic consequences. Mild, horseshoe-shaped uptake in the suprapatellear bursa above total knee prostheses and focal uptake around the neck of total hip prostheses (outside the osseous structures) were interpreted as negative for infection because these represent clinically insignificant sterile inflammation, as was described by Nijhof et al. (*24*). Positive scintigraphic findings were classified as false-positive if they did not account for the diagnostic problem, even if signs or symptoms of inflammation could be detected.

The highly similar biodistributions of ^{99m}Tc-HYNIC–IgG and ^{111}In–IgG in this study are in agreement with the findings of Callahan et al. (*28*), who found similar imaging and biodistribution properties of the two radiopharmaceuticals in normal human subjects. Accumulation of radiolabeled proteins in infectious and inflammatory foci appears to be partly determined by the radionuclide and labeling method (*21*). Indium-111–IgG is thought to extravasate in inflammatory areas by virtue of increased vascular permeability, with subsequent retention of the radionuclide (*29*). Our clinical results suggests a similar mechanism of inflammation localization for ^{99m}Tc-HYNIC–IgG, as recently indicated in experimental infection (*30*).

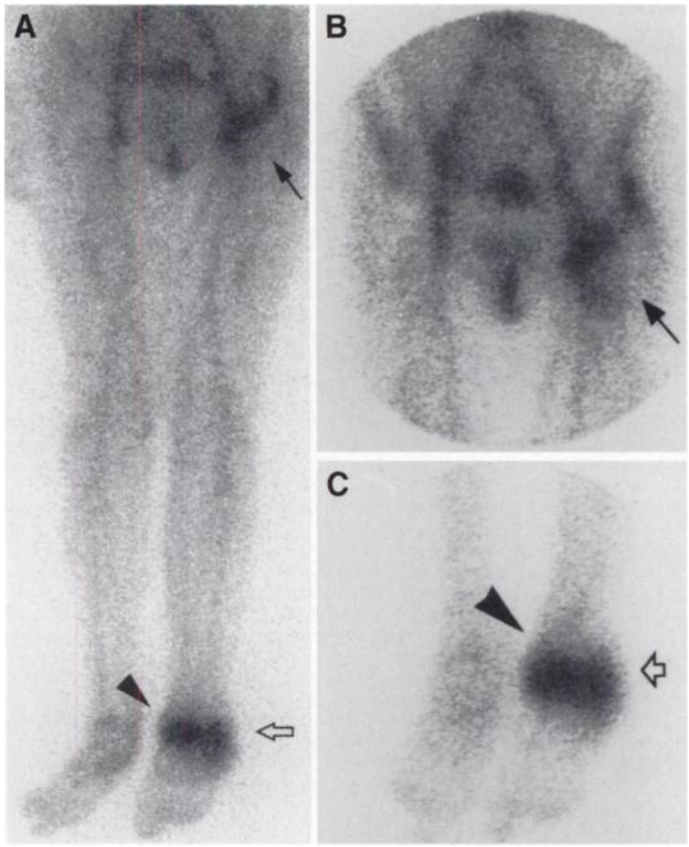

FIGURE 3. Patient 9 (female, age = 40 yr), who has severe rheumatoid arthritis, had a 2-wk history of fever and increasing pain in left ankle, heel and left total hip prosthesis. Cultures from needle aspiration grew *Staphylococcus aureus*. Technetium-99m-HYNIC–IgG scintigram at 24 hr postinjection, (A) anterior whole-body view, and ^{111}In–IgG scintigram at 24 hr postinjection, spot views of the (B) pelvis and (C) lower legs. Both scans show increased uptake around the prosthesis (solid arrow), the foot (open arrow) and ankle (arrowhead).

A potential disadvantage of a radiopharmaceutical labeled with ^{99m}Tc in detecting chronic infections is its short half-life, which limits imaging beyond 24 hr. In the present series of patients, however, all chronic infections were adequately delineated within 24 hr postinjection The slow blood clearance of ^{99m}Tc-HYNIC–IgG resulted in persisting background activity, but this did not interfere with the interpretation of the 24-hr images.

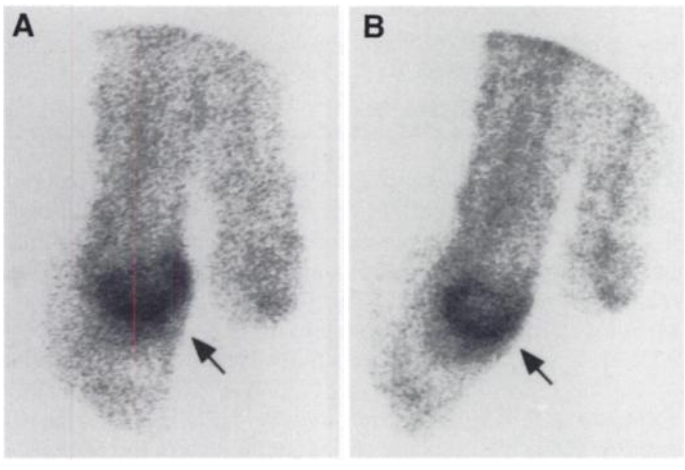

FIGURE 4. Concordantly positive ^{99m}Tc-HYNIC–IgG and ^{111}In–IgG scintigrams of Patient 2 (male, age = 45 yr), who had congenital clubfeet and an infected wound on the right foot for 2 mo before presentation. Focal accumulation is seen in the talus with soft-tissue extension (arrows). Samples taken at surgery grew *Pasteurella multocida*. (A) Technetium-99m-HYNIC–IgG scintigram and (B) ^{111}In-DTPA–IgG scintigrams, both showing spot views of the lower legs, at 24 hr postinjection.

Other techniques for labeling IgG with ^{99m}Tc have been studied, but several problems are encountered. The iminothiolane-labeling method, as used in the ^{99m}Tc-HIG preparation (*31*), leads to instability toward transchelation, which probably accounts for the relatively fast blood clearance (*20*). Although this results in lower background activity compared to the ^{99m}Tc-HYNIC–IgG, the rapid clearance limits IgG diffusion into the inflammatory areas, resulting in decreased target uptake (*23*). In addition, the iminothiolane-based ^{99m}Tc–IgG preparations showed marked accumulation in the kidney, both in experimental (*20,23*) and in clinical studies (*32,33*). This enhanced kidney uptake is probably related to the transchelation toward free sulph-hydryl-containing metabolites, which are known to be retained in the renal cortex (*34*). Furthermore, physiological excretion into the colon has been reported, which compromises adequate imaging of abdominal infections (*35,36*). In an experimental comparative study, ^{99m}Tc-HYNIC–IgG was found to have higher in vivo stability, lower kidney uptake and the highest retained activity in the abscess compared to both ^{99m}Tc-2-iminothiolane–IgG and ^{99m}Tc–IgG labeled according to the (direct) Schwarz method (*23*). As in this study, Callahan et al. (*28*) reported low concentrations of both ^{111}In–IgG and ^{99m}Tc-HYNIC–IgG in the gastrointestinal tract, suggesting that ^{99m}Tc-HYNIC–IgG might be a suitable agent for scintigraphic evaluation of patients suspected of infection and/or inflammation in the abdomen. Another method, labeling ^{99m}Tc to IgG through a diamino dimercaptide chelator, also has high in vivo stability (*19*). The procedure, however, is relatively complicated (hot conjugation, >2 hr preparation). Labeling ^{99m}Tc to the HYNIC–IgG conjugate is rapid and efficient. When tricine is used as an intermediary ligand, more than 95% labeling efficiency is achieved within 15 min at room temperature (*37*).

In this study, there were no patients with acute and parenchymatous infection. According to the literature, ^{111}In–IgG imaging can adequately detect these infections (*14,25,27*). Technetium-99m-HYNIC–IgG is very likely to show a similar performance and is theoretically more suitable for evaluation of acute infections. However, this remains to be proven in further studies.

CONCLUSION

This study indicates that ^{99m}Tc-HYNIC–IgG scintigraphy is equally as effective as ^{111}In–IgG scintigraphy for detection of nonacute infection and inflammation. The more favorable imaging and physical properties of ^{99m}Tc, the greater availability and lower cost make ^{99m}Tc-HYNIC–IgG a promising new radiopharmaceutical for imaging of infection and inflammation.

ACKNOWLEDGMENTS

We thank A. Meeuwis and his staff and E. Koenders for their technical assistance.

REFERENCES

1. Hoffer P. Gallium and infection. *J Nucl Med* 1980;21:484–488.
2. Staab EV, McCartney WH. Role of gallium-67 in inflammatory disease. *Semin Nucl Med* 1978;8:219–234.
3. McAfee JG, Thakur ML. Survey of radioactive agents for the in vitro labeling of phagocytic leukocytes. *J Nucl Med* 1976;17:480–492.
4. Segal AW, Arnot RN, Thakur ML, Lavender JP. Indium-111-labeled leukocytes for localisation of abscesses. *Lancet* 1976;ii:1056–1058.
5. Froelich JW, Swanson D. Imaging of inflammatory processes with labeled cells. *Semin Nucl Med* 1984;14:128–140.
6. Peters AM, Danpure HJ, Osman S, et al. Preliminary clinical experience with Tc-99m-HMPAO for labelling leucocytes and imaging infection. *Lancet* 1986;ii:945–949.

7. Vorne M, Soini I, Lantto T, Paakkinen S. Technetium-99m-HMPAO-labeled leukokytes in detection of inflammatory lesions: comparison with gallium-67-citrate. *J Nucl Med* 1989;30:1332–1336.
8. Perkins PJ. Early gallium-67 abdominal imaging: pitfalls due to bowel activity. *Am J Roentgenol* 1981;136:1016–1017.
9. Datz FL. Abdominal abscess detection: gallium, ^{111}In-, and ^{99m}Tc-labeled leukocytes, and polyclonal and monoclonal antibodies. *Semin Nucl Med* 1996;26:51–64.
10. Ebright JR, Soin JS, Manoli RS. The gallium scan. Problems and misuse in examination of patients with suspected infection. *Arch Intern Med* 1982;142:246–254.
11. Seabold JE, Nepola JV, Conrad GR, et al. Detection of osteomyelitis at fracture nonunion sites: comparison of two scintigraphic methods. *Am J Roentgenol* 1989;152: 1021–1027.
12. Bekerman C, Hoffer PB, Bitran JD. The role of gallium-67 in the clinical evaluation of cancer. *Semin Nucl Med* 1984;14:296–323.
13. Lange JMA, Boucher CAB, Hollak CEM, et al. Failure of zidovudine prophylaxis after accidental exposure to HIV-1. *N Engl J Med* 1990;322:1375–1377.
14. Rubin RH, Fischman AJ, Callahan RJ, et al. In-111-labeled nonspecific immunoglobulin scanning in the detection of focal infection. *N Engl J Med* 1989;321:935–940.
15. Serafini AN, Garty I, Vargas-Cuba R, et al. Clinical evaluation of a scintigraphic method for diagnosing inflammations/infections using indium-111-labeled nonspecific human IgG. *J Nucl Med* 1991;32:2227–2232.
16. Datz FL, Anderson CE, Ahluwalia R, et al. The efficacy of indium-111-polyclonal IgG for the detection of infection and inflammation. *J Nucl Med* 1994;35:74–83.
17. Khalkali I, Mena I, Rauh DA, Diggles LE, Pham HL, Mason GR. 111-Indium-DTPA-IgG lung imaging in patients with pulmonary and HIV infection. *Chest* 1995;107: 1336–1341.
18. Oyen WJG, Claessens RAMJ, Raemaekers JMM, de Pauw BE, van der Meer JWM, Corstens FHM. Diagnosing infection in febrile granulocytopenic patients with indium-111 labeled human IgG. *J Clin Oncol* 1992;10:61–68.
19. Fritzberg AR, Abrams PL, Beaumier PL, et al. Specific and stable labeling of antibodies with technetium-99m with a diamide dithiolate chelating agent. *Proc Natl Acad Sci USA* 1988;85:4025–4029.
20. Hnatowich DJ, Mardirossian G, Rusckowski M, Fogarasi M, Virzi F, Winnard P Jr. Directly and indirectly technetium-99m-labeled antibodies: a comparison of in vitro and animal in vivo properties. *J Nucl Med* 1993;34:109–119.
21. Oyen WJG, Claessens RAMJ, van der Meer JWM, Corstens FHM. Biodistribution and kinetics of radiolabeled proteins in rats with focal infection. *J Nucl Med* 1992;33:388–394.
22. Abrams MJ, Juweid M, ten Kate CI, et al. Technetium-99m-human polyclonal IgG radiolabeled via the hydrazino nicotinamide derivative for imaging focal sites of infection in rats. *J Nucl Med* 1990;31:2022–2028.
23. Claessens RAMJ, Boerman OC, Koenders EB, Oyen WJG, van der Meer JWM, Corstens FHM. Technetium-99m labelled hydrazinonicotinamido human non-specific polyclonal immunoglobulin G for detection of infectious foci: a comparison with two other technetium-labelled immunoglobulin preparations. *Eur J Nucl Med* 1996;23: 414–421.
24. Nijhof MW, Oyen WJG, van Kampen A, Claessens RAMJ, van der Meer JWM, Corstens FHM. Evaluation of infections of the locomotor system with indium-111-labeled human IgG scintigraphy. *J Nucl Med* 1997;38:1300–1305.
25. Oyen WJG, Claessens RAMJ, van der Meer JWM, Corstens FHM. Detection of subacute infectious foci with indium-111-labeled autologous leukocytes and with indium-111-labeled human nonspecific immunoglobulin G: a prospective comparative study. *J Nucl Med* 1991;32:1854–1860.
26. Arka A, Aktolun C, Gooden C, Epenetos A, Papadimitriou A. Tc-99m-labeled nonspecific polyclonal human immunoglobulin G is taken up by malignant tumors. *Clin Nucl Med* 1994;19:708–712.
27. Fischman AJ, Rubin RH, Khaw BA, et al. Detection of acute inflammation with In-111 labeled nonspecific polyclonal IgG. *Semin Nucl Med* 1988;18:335–344.
28. Callahan RJ, Barrow SA, Abrams MJ, Rubin RH, Fischman AJ. Biodistribution and dosimetry of technetium-99m-hydrazino nicotinamide IgG: comparison with indium-111-DTPA-IgG. *J Nucl Med* 1996;37:843–846.
29. Corstens FHM, Oyen WJG, Becker WS. Radioimmunoconjugates in the detection of infection and inflammation. *Semin Nucl Med* 1993;23:148–164.
30. Claessens RAMJ, Koenders EB, Oyen WJG, Corstens FHM. Retention of technetium-99m in infectious foci in rats after release from technetium-99m labelled human non-specific polyclonal immunoglobulin G: a dual study with hydrazinonicotinamido and iminothiolano immunoglobulin. *Eur J Nucl Med* 1996;23:1536–1539.
31. Goedemans WT, Panek KJ. A new method for labeling with ^{99m}Tc [Abstract]. *J Nucl Med Allied Sci* 1989;33:286.
32. Hovi I, Taavitsainen M, Lantto T, Vorne M, Paul R, Remes K. Technetium-99m-HMPAO-labeled leukocytes and technetium-99m-labeled human polyclonal immunoglobulin G in diagnosis of focal purulent disease. *J Nucl Med* 1993;34:1428–1434.
33. Buscombe JR, Lui D, Ensing G, de Jong R, Ell PJ. ^{99m}Tc-human immunoglobulin (HIG): first results of a new agent for the localization of infection and inflammation. *Eur J Nucl Med* 1990;16:649–655.
34. Moretti JL, Rapin JR, Saccavini JC, Lageron A, Le Poncin M, Bardy A. 2,3-Dimercaptosuccinic acid chelates: their structure and biological behaviour. In: Raynaud C, ed. *Proceedings of the Third World Congress of Nuclear Medicine and Biology.* Paris: Nuclear Medicine and Biology; 1982:1651–1654.
35. Spinelli F, Milella M, Sara R, Banfi F, Possa M, Vigorelli R. The value of Tc-99m-labelled human immunoglobulin scan in the evaluation of Crohn's disease. *Nucl Med* 1990;27:274–278.
36. Arndt JW, van der Sluys-Veer A, Blok D, et al. A prospective comparison of Tc-99m-labeled polyclonal human immunoglobulin and In-111 granulocytes for localization of inflammatory bowel disease. *Acta Radiol* 1992;33:140–144.
37. Larsen SK, Caldwell G, Higgins III JD, Abrams MJ, Solomon HF. Technetium complex of tricine: useful precursor for the ^{99m}Tc-labelling of hydrazino nicotinamide modified proteins [Abstract]. *J Labelled Compd Rad* 1994;35:1–2.

Iterative Reconstruction of Fluorine-18 SPECT Using Geometric Point Response Correction

Gengsheng L. Zeng, Grant T. Gullberg, Chuanyong Bai, Paul E. Christian, Frederick Trisjono, Edward V.R. Di Bella, Jared W. Tanner and Hugh T. Morgan

University of Utah, Salt Lake City, Utah; and Picker International, Inc., Cleveland, Ohio

This article demonstrates resolution recovery in ^{18}F SPECT image reconstruction by using an iterative algorithm that corrects for the system geometric response. **Methods:** Patient and phantom studies were performed using a Picker PRISM 3000 three-detector SPECT system (Picker International, Inc., Cleveland, OH) to image ^{18}F with 511 keV collimators. A measured point response function of the imaging system was used in an iterative reconstruction algorithm in which the projector and backprojector modeled the system point response function by using an efficient layer-by-layer blurring technique. The blurring function was a five-element kernel in the shape of a cross. The iterative reconstruction algorithm was an ordered-subset maximum-likelihood expectation maximization algorithm. **Results:** The iterative reconstruction algorithm with geometric response correction showed an improvement in resolution over the filtered backprojection reconstruction and the iterative reconstruction without correction. **Conclusion:** The proposed iterative reconstruction algorithm with geometric response correction is efficient and effective with significant resolution recovery.

Received Sep. 23, 1996; revision accepted Apr. 11, 1997.

For correspondence or reprints contact: Grant T. Gullberg, PhD, Department of Radiology, 729 Arapeen Dr., University of Utah, Salt Lake City, UT 84108-1218.

Key Words: fluorine-18-fluorodeoxyglucose; SPECT; geometric point response correction

J Nucl Med 1998; 39:124–130

Recent efforts have used SPECT systems for imaging positron emitters such as ^{18}F. The reason has been that ^{18}F-FDG is so effective in imaging metabolism that it gives high-contrast images between viable and nonviable tissue and between malignant and benign tissue. The problem with SPECT imaging of 511 keV photons is low sensitivity due to poor geometric efficiency and poor crystal sensitivity and poor resolution due to the need for thick septum and large holes in 511 keV collimators. It is hypothesized that by modeling the spatially varying geometric response of these collimators the resolution of reconstructed SPECT images can be improved, and it may be comparable to results obtained with lower energy radiopharmaceuticals commonly used in clinical nuclear medicine.

Imaging with radioactive fluorine was first performed more than 30 yr ago. In 1962, Blau et al. (*1*) used a small scintillation probe to acquire images of the uptake of ^{18}F in bone. In 1965,